17th World Conference on Earthquake Engineering, 17WCEE
Sendai, Japan - September 13th to 18th 2020

BUILDING DAMAGE DETECTION USING POST-SEISMIC UAV DATA

X.H. Zhang[(1)], X.X. Du [(2)], J.Y. Lai [(3)], X.Q. Wang [(4)]

[(1)] *Assistant Engineer, National Earthquake Response Support Service, zhangxhua1990@163.com*
[(2)] *Senior Engineer, National Earthquake Response Support Service, junyalai@126.com*
[(3)] *Senior Engineer, National Earthquake Response Support Service, duxx_bj@126.com*
[(4)] *Professor, Institute of Earthquake Forecasting, China Earthquake Administration, wangxiaoq517@163.com*

Abstract

In recent years, the development of UAV (Unmanned Aerial Vehicle) remote sensing technology has provided strong conditions for the rapid acquisition of post-seismic images, and also promoted the research on the method of extracting earthquake information. Many studies have showed that the accuracy of building extraction that combined high resolution remote sensing image with three-dimensional (3D) laser radar point cloud data is much higher than that of single data. However, the data obtained by laser radar is limited by the time efficiency and economy. In order to break through this limits, this paper presents a building damage extraction method that based on the UAV high resolution remote sensing image and its dense point cloud data. The proposed method was tested in the Beichuan earthquake ruins, Sichuan province, China, that the significant disaster area of Wenchuan Earthquake (2008). The method is mainly divided into three steps :(1) using UAV to obtain high-resolution remote sensing images of the study area, and to obtain the DOM (Digital Orthophoto Map) and its point cloud data that through the processing ,such as SfM (Structure from Motion) and MVS(Multi-View-Stereo);(2) to extract and process the point cloud data to obtain non-ground points;(3) using the object-oriented image analysis method to extract the damage information of buildings with the high resolution DOM and its point cloud data, and then divided the seismic damage buildings into two categories, namely collapsed and not collapsed, comparing the results with the visual interpretation results and using kappa coefficient for accuracy assessment. The experimental results show that the method can not only quickly acquire the information of earthquake disaster, but also improved the accuracy of seismic building damage extraction compared with the high resolution remote sensing only.

Keywords: UAV; point cloud; Object-oriented; building damage extraction; Wenchuan earthquake (2008);

1. Introduction

A large number of buildings will be collapsed in an instant when a major earthquake disaster occurs. To obtain the disaster information quickly and accurately after earthquake is an important guarantee for implementing effective emergency rescue and minimizing the loss of earthquake disaster [1]. Due to the advantages of large observation rang, abundant information, multiple technical segments, and short update period, remote sensing technology has become one of the main methods for quickly obtaining earthquake damage information [2]. Generally, there have three types of remote sensing platform for to obtain high-resolution images of large areas: satellites, manned aircraft, and unmanned aerial vehicles (UAVs) [3]. UAVs can be deployed quickly and repeatedly, and can acquire data in high-risk areas whiles reducing the risk of personal, but the flight cover areas is limited due to battery duration [4]. However, as UAVs is flying at low altitude that close to the target objects, it can acquire images with high resolution and get more detailed information [5,6]. With the advent and availability of accurate and miniature global navigation satellite systems (GNSS) and inertial measurement units (IMU), as well as the availability of premium consumer digital cameras and other miniature sensors, UAVs technology has had developing rapidly in many areas, such as agricultural surveys, power line inspections, disaster assessments [7,8].

Until to now, the development of remote sensing image information extraction models has the following three stages: from 1960s to 1980s, statistical modeling techniques was used for remote sensing data analysis, and defined a “digital signal processing era”; in the 1990s, remote sensing science and technology entered a “quantitative remote sensing era”, and physical modeling techniques was the mainly information extraction approach; in recent years, the concept of big data has been proposed, which has promoted the development of artificial intelligence algorithms such as deep learning, and remote sensing data information extraction technologies are gradually entering a “remotely sensed big data era”, which is characterized by intelligent information extraction [9-11]. As we all know, deep learning models have great application prospects in remote sensing information extraction, but the number of available training samples is limited. However, the samples is unavailable of building damage after earthquake occurred immediately. Many researchers have studied remote sensing information extraction methods combining remote sensing data with others. Based on the different performance characteristics of building damage in optical, synthetic aperture radar (SAR), light detection and ranging (LiDAR), the multi-source remote sensing data joint analysis was considered of building seismic damage information extraction, and the information extraction result of multi-data was better than using a single data [12]. Because LiDAR data has three-dimensional information, a large number of studies have shown that the combination of point cloud data and images can improve the accuracy of information extraction of remote sensing image. However, due to the limits of road conditions of the affected area and the portability of equipment, there are still some limitations in obtaining radar data as soon as possible after the earthquake. And multi-source means that multiple sensors were used to acquisitions for the same area as a result of wasting a lot of time.

This paper presents a building damage extraction method that based on the UAV high resolution remote sensing image and its dense point cloud data, which only needs to flight once with UAV equipped with optical camera and saves time greatly. Many studies have confirmed that point cloud data generated by drone optical images is basically the same as that of LiDAR point cloud data [13-16]. So we don’t verify the accuracy of the point cloud data. The method is mainly divided into three steps:(1) using UAV to obtain high-resolution remote sensing images of the study area, and to obtain the DOM (Digital Orthophoto Map) and its point cloud data that through the processing ,such as SfM (Structure from Motion) and MVS(Multi-View-Stereo);(2) to extract and process the point cloud data to obtain non-ground points, and to evaluate the accuracy;(3) using the object-oriented method to extract the damage information of buildings with the high resolution DOM and its point cloud data, and then divided the seismic damage buildings into two categories, namely collapsed and not collapsed, comparing the results with the visual interpretation results and using kappa coefficient for accuracy assessment.

2. Methods

The framework for the acquisition and processing of UAV images in the study areas consists of five main parts, *i.e.*, flight route design, image acquisition and matching, DOM and point cloud data generation, and point cloud data processing and 3D feature extraction, building damage information detection. Fig.1 shows the entire technological framework of the study. In the first step, the design of the flight route is based on specific factors for photogrammetric and aerial image orientation for the UAV, as well as flight safety and minimum flight time. In the second part, both UAV images and the position and orientation system (POS) data are acquired during autonomous flight operations, and the scale-invariant feature transform (SIFT) operator [17] and the random sample consensus (RANSAC) approach [18] are used in the conjugate point extraction and the outliers identify and eliminate. In the third part, the Multi-View Stereo (MVS) was used for to encrypt the point cloud, based on the conjugate point from the second part, and the DOM was generated. In the fourth step, in order to improve the accuracy of the calculation of the 3D feature of the point cloud, the point cloud gridding operation was used, and then the value of the slope of the roof was calculated. In the last part, the DOM and the slope value result was used for building damage information extraction.

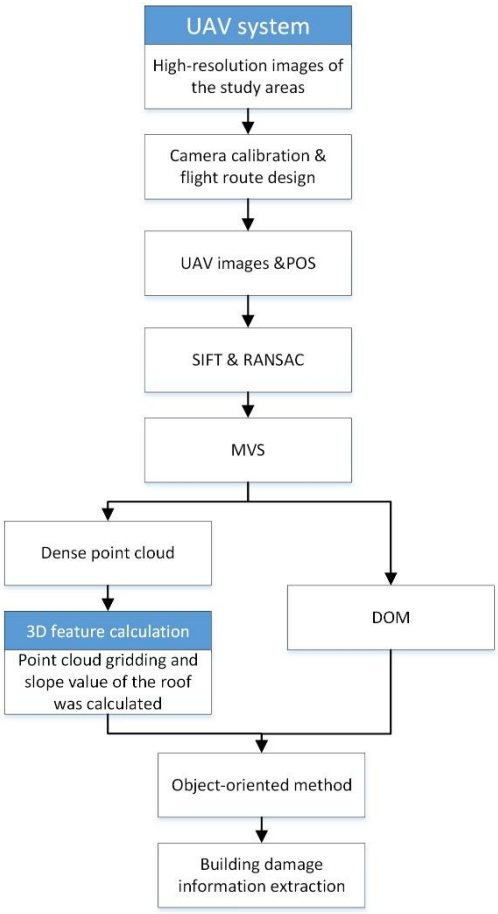

Fig. 1 – Entire workflow of the study

2.1 Materials and data acquisition

2.1.1 The UAV system and sensors

The UAV system used in this study is an F1000 fixed UAV manufactured by the Shenzhen Feima Robotics Co., Ltd. The system consists of two main components: aerial and ground systems (Fig.2). The aerial systems include the remote sensing camera, the automatic control system and the UAV platform. The main functions

of the aerial systems are to flight along the route that uploaded by the ground system while acquisition the ground image, and monitor and return the status of the UAV. The ground systems consist of the ground station that planning the flight routes and receive the UAV status information, and wireless transmission system. The main functions of the ground systems are to design and schedule the flight routes, and record the location when taking photos.

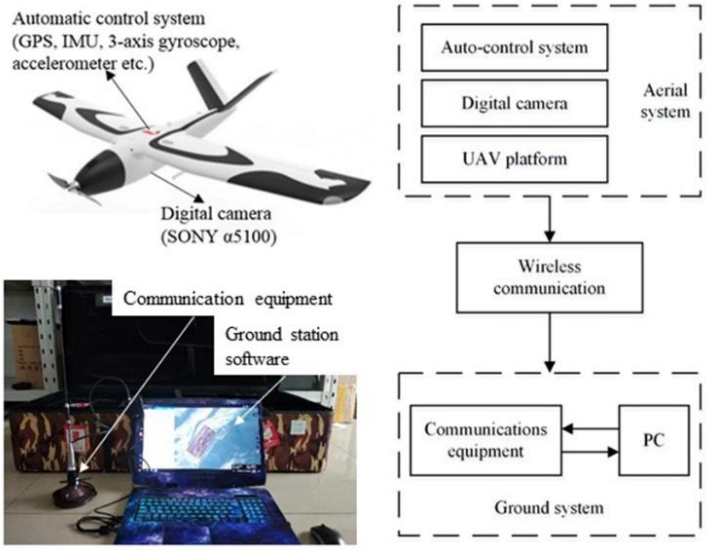

Fig. 2 – The UAV system used in the experiment

Table 1 shows the technical specifications of the UAV platform and the mounted digital camera. The automatic control systems can realize automatic navigation and real-time monitoring of the overlooked areas. And the UAV can fly automatically, according to the predefined flight routes. Take photos at set intervals or distances during the flight, the spatial location of the UAV and three attitude angles are recorded.

Table 1 – Technical specifications of the UAV platform and the mounted camera in the experiment

	Item	**Value**
UAV platform	**Length (m)**	1.1
	Wingspan (m)	1.6
	Take-off weight (kg)	3
	Endurance (h)	1.5
	Flying height (m)	6000
	Flying speed (km/h)	60
	Capacity	Electric
	Sensor	Digital camera
	Launch	Hand throw
	Landing	Sliding, parachute
	Flight mode	autonomous

Digital camera	**Sensor size (mm)**	APS-C 23.5*15.6
	Effective pixels(million)	24.3

2.1.2 Study area and data acquisition

The study area is located in the Beichuan qiang autonomous county, Sichuan province, China, and was severely damaged by the Wenchuan M_s8.0 earthquake on May 12, 2008 (Fig.3), and protected as an earthquake site.

Prior to the image acquisition, flight route and heights, image overlap was designed in the ground station software on PC. And UAV remote sensing data acquisition was performed on December 16, 2016, a total of 215 UAV images were collected over the study areas. The spatial resolution of these UAV images is approximately 6cm, with 80% forward and side lap. The UAV images were acquired during the flight and stored on the camera's 64GB memory card. For each image, the corresponding shooting time, GPS, roll, pitch and heading information were recorded. Images and flight data were downloaded after landing and the quality is checked firstly. The work of images mosaic and DOM and dense point cloud generation were completed using Agisoft PhotoScan Professional software (https://www.agisoft.com/), which is not described in this article.

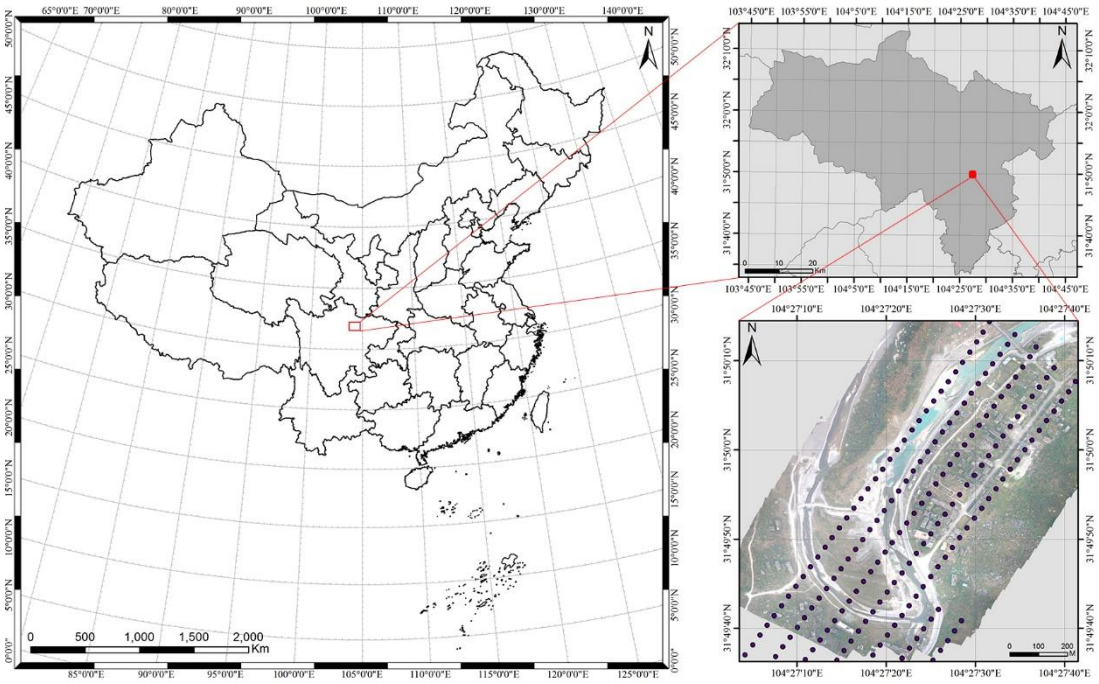

Fig. 3 – The study areas in the experiment

2.2 Point cloud processing

Densen point cloud data is generated by UAV images using SIFT and MVS algorithm, and there are noisy points and a lot of ground object side points. Firstly, we process the point data in order to make better use of the 3D information of building point. The point processing flow is shown in Fig.4 in order to obtain the building point. Noisy points are easier to find, and removed by manual. The process of removing abnormal points caused by flying objects such as birds and measurement errors in point cloud data is called point cloud denoising, and usually can be removed manually. Point filtering is to separate ground and nonground points. After decades of research and development, many high-quality point filtering algorithms have been formed [19-20]. After comparison of multiple methods, we chooses Cloth Simulation Filtering (CSF) algorithm for point cloud filtering [21]. About to removal vegetation point in the data, we have investigated a large number of methods. The currently commonly used method is the vegetation index method, such as Normalized

Difference Index (NDI), Excess Greed (EXG), Normalized Greed-Red Difference Index (NGRDI), Visible-Band Difference Vegetation Index (VDVI) [22-25], and VDVI (Eq. (1)) was used in the paper.

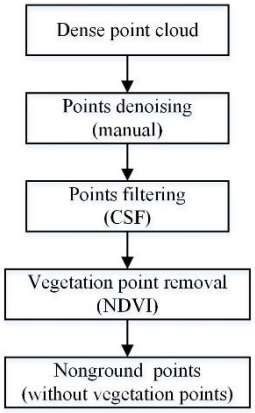

Fig. 4 – The flow of point cloud processing

$$\mathrm{VDVI} = \frac{2*\rho_{green}-(\rho_{red}+\rho_{blue})}{2*\rho_{green}+(\rho_{red}+\rho_{blue})} \quad (1)$$

In the Eq. (1), ρ represents the values in different bands.

2.3 3D feature extraction

From the method of point cloud generation, it can be known that the data has the disadvantages of uneven density and error distribution, which will affect the accuracy of the 3D feature of the building. About the slope feature, only the roof point is needed of the building, so we must find a way to reduce the impact of the side point. Therefore, we conducts grid processing for the point cloud firstly. After many experiments, the result of the slope was the best using points with an elevation value distribution greater than 1 standard deviation in the grid, and can basically eliminate the effects of points on the side of the building (Fig.5).

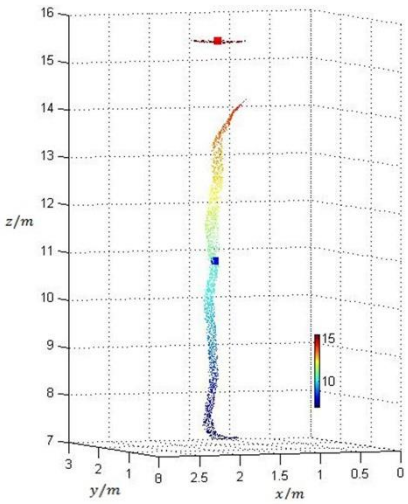

Fig. 5 – The sketch map of point cloud data gridding

(The red squares represent the point in the grid that calculated using 1 standard deviation points; the blue squares represent the point in the grid that calculated using all points in the grid.)

The slope between adjacent point clouds on the intact building roof has regularity. After the building collapses, the point cloud distribution is scattered and the height distribution is changed, and the slope value

will change accordingly. This feature can be used to collapse and not collapse division of buildings. Slope value calculation principle: The calculation is performed by searching for the point closest to the plane of the target point, and the calculation formula is shown in Eq. (2).

$$S = \frac{|z_1 - z|}{\sqrt{(x_1 - x)^2 + (y_1 - y)^2}} \tag{2}$$

In the Eq. (2), $p_1(x_1, y_1, z_1)$ is the nearest neighbor projected by $p(x, y, z)$ onto the 2D plane.

2.4 Building damage extraction

With regard to extracting building damage information, the object-based image analysis (OBIA) method is suitable for high–resolution images and has been demonstrated in many studies [5, 26-28]. In the experiment, the OBIA method was developed in software. In this experience, the main steps of building damage information extraction are three: (1) DOM, nDSM (Normal Digital Surface Model) and slope feature images were segmented by the multi-scale segmentation algorithm; (2) Select feature parameters and metrics to extract building damage information based on decision tree; (3) Determining the accuracy of building damage information classification (Fig.6).[29]

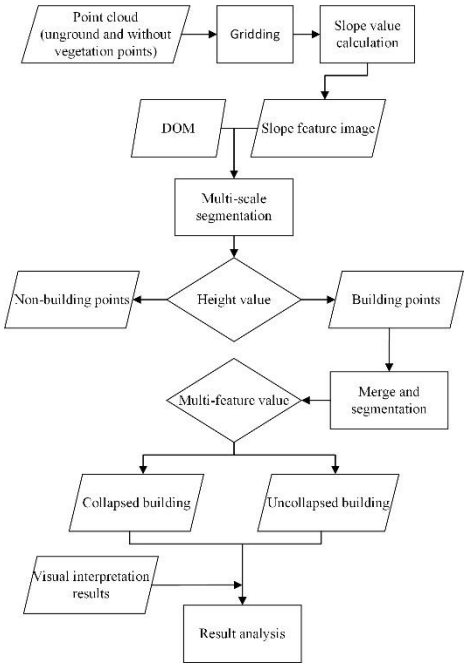

Fig. 6 – The flow of building damage extraction and classification

3. Result and discussion

3.1 Results of building damage classification

It is a key point to obtain remote sensing images of the affect area quickly and accurately extract building damage information and classification after the earthquake. It can not only provide a basis for decision-making for commanders, but also provide a useful reference for rescue teams and the distribution of rescue supplies. And we divided building damage information into two categories: collapsed buildings and uncollapsed buildings. Due to the high spatial resolution of the UAV images, visually interpretation results of building damage classification were used as reference results, and total of 177 buildings were interpreted of which 78 collapsed buildings and 99 uncollapsed building. And in this experiment, a total of 168 buildings were extracted of which 73 collapsed and 95 uncollapsed. Fig.7 shows the results of the building damage

classification in the experiment and the visually interpretation results in the study areas. Table 2 shows the accuracy evaluation of experimental classification.

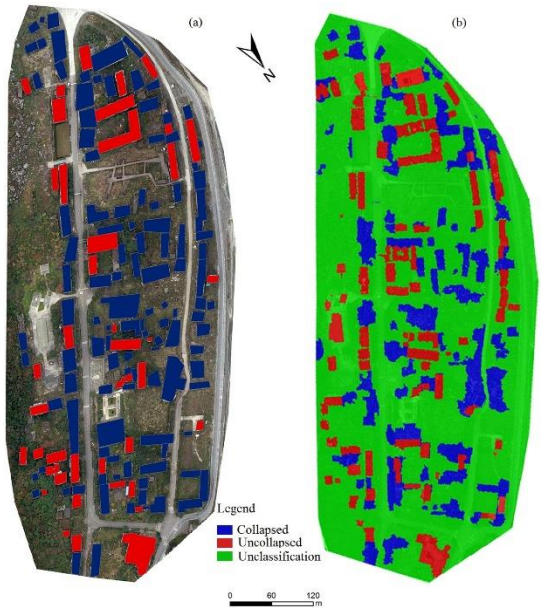

Fig. 7 – The results of building damage extraction and classification

(a) Visually interpretation results; (b) Experimental results.

Table 2 – Evaluation for the accuracy of experimental classification and visual interpretation results

		Visual interpretation		Total
		Collapsed building	Uncollapsed building	
Experimental classification	Collapsed building	61	12	73
	Uncollapsed building	15	80	95
Total		76	92	168

Based on the above results, the overall classification accuracy (OA) and the Kappa coefficient of this experimental method can be calculated. OA was 83% and Kappa was 0.67.

3.2 Discussion

In this study, we described a method for extracting buildings seismic damage after earthquake, using optical images obtained from one flight of UAV to process the DOM and 3D feature images of the study area. The mainly steps are: (1) the SfM and MVS methods were used for obtain the DOM and its dense point cloud using the high-resolution remote sensing optical images of UAV, and it was finished in the software; (2) in order to use the 3D characteristics of point cloud data more effectively, the point cloud processing was performed in this step (section 2.2) and the nDSM was obtained but not proposed in the text, and the slope feature image of building was obtained (section 2.3). (3) OBAI method was used in this study to extract the building damage information with the high-resolution DOM, nDSM and slope feature image. In this experiment, the height value and slope feature were important because many non-building objects can be remove before the building damage information extracted. Buildings damage were divided into two categories: collapsed and not collapsed.

From the results of this experimental method in Table 2, we can see that 61 collapsed building and 80 collapsed building were extracted. The overall accuracy of the classification of the building damage information was 83%, and it's better than using DOM only. But about the experience, there are three issues that need to be discussed as follow:

(1) Using the UAV remote sensing images to generate dense point cloud data effectively reduces the data acquisition time and avoids the problem of matching between multiple data. Based on previous studies of others, we didn't to verify the accuracy of the dense point cloud in this experience. Even if the dense point cloud data has a certain accuracy error, the error is smaller after we gridize the point cloud data. As the same time, there is no data matching problem between DOM and point data.

(2) In the accuracy evaluation, we use the building objects to evaluate the experimental results, without considering the object boundary issues. At the same time, it did not consider the problem of misclassification of results, which resulted in higher classification accuracy.

(3) Many studies had proposed new methods that can achieve higher accuracy of building seismic damage extraction using high-resolution data of drone or very high resolution satellite images [30,31]. And each method has its own data adaptability and regional adaptability, and does this method. This paper did not conduct experiments in other regions, and the accuracy of the results may be inconsistent.

4. Conclusion

This paper proposes a framework for building seismic damage extraction based on UAV remote sensing optical images. Use the UAV platform to fly once to obtain the optical and point cloud data in the study area, reduced the data acquisition time, and improve the accuracy of building damage extraction and classification. The results showed that: (1) we can get two types data quickly, especially in emergency time after disaster. This method reduces the flying time of the drone, acquires the elevation data of the ground objects, while avoids the disadvantages of the radar equipment; (2) the result showed that this was an acceptable accuracy during the rapid post-seismic evaluation phase, but there are some problems with this method as mentioned in section 3.2; (3) although there are some problems with our accuracy evaluation, this framework can meet the needs for disaster command and decision-making.

5. Acknowledgements

The research was supported by National Key R&D Program China (No. 2017YFB0504104).

6. Copyrights

7. References

[1] Wang XQ, Dou AX, Wang L, Yang XX, Ding X, Zhang W. (2015): RS-based assessment of seismic intensity of the 2013 Lushan, Sichuan, China M_S7.0 earthquake. *China J. Geophys*, **58** (1), 163-171. *(in Chinese)*

[2] Liu JH, Yang JF, Wei CJ, Guan ZQ. (2004): Acquisition of earthquake damage information based on remote sensing technology: History, current situation and trend. *Journal of Natural Disasters*, **13**(5), 46-52. *(in Chinese)*

[3] Tong XH, Liu XF, Chen P, et al. (2015): Integration of UAV-based photogrammetry and terrestrial laser scanning for the three-dimensional mapping and monitoring of open-pit mine areas. *Remote Sensing*, 7, 6635-6662.

[4] Eisenbeiss H. (2009): UAV Photogrammetry. Ph.D. Thesis, University of Technology Dresden, Dresden, Germany.

[5] Laliberte AS, Rango A. (2009): Texture and scale in object-based analysis of subdecimeter resolution unmanned aerial vehicle (UAV) imagery. *IEEE Transactions on Geoscience and Remote Sensing*, **47**(3), 761-770.

[6] Zhang YJ, Xiong JX, Hao LJ. (2011): Photogrammetric processing of low-altitude images acquired by unpiloted aerial vehicles. *Photogramm. Rec*, 26,190-211.

[7] Zhou GQ. (2010): Geo-referencing of video flow from small low-cost civilian UAV. *IEEE Trans. Autom. Sci. Eng.* 7,156-166.

[8] Turner D, Lucieer A, Watson C. (2012): An automated technique for generating georectified mosaics from ultra-high resolution unmanned aerial vehicle (UAV) imagery, based on structure from motion (SfM) point clouds. *Remote Sens.* 4, 1392-1410.

[9] Zhang B, Chen ZC, Peng DL, et al. (2019): Remotely sensed big data: Evolution in model development for information extraction. *Proceedings of the IEEE*. **107**(12), 2294-2301.

[10] Hogg J. (2004): Quantitative remote sensing of land surface. *Photogrammetric Record.* **19**(108), 413-422.

[11] Chi M, Plaza A, Benediktsson JA, et al. (2016): Big data for remote sensing: Challenges and opportunities. *Processing of the IEEE.* **104**(11), 2207-2219.

[12] Su YY. (2015): Building damage analysis and extraction from multi-source remote sensing data. The institute of crustal dynamics, CEA. Master degree. *(in Chinese)*

[13] James MR, Robson S. (2012): Straightforward reconstruction of 3D surfaces and topography with a camera: Accuracy and geoscience application. *Journal of Geophysical Research.* **117**(F03017). doi:10.1029/2011JF002289.

[14] Chiabrando F, Nex F, Piatti D, Rinaudo F. (2011): UAV and RPV systems for photogrammetric surveys in archaeological areas: Two tests in the Piedmont region (Italy). *J. Archaeol. Sci.* 28,697-710.

[15] Zhang YJ, Xiong JX, Hao LJ. (2011): Photogrammetric processing of low-altitude images acquired by unpiloted aerial vehicles. *Photogramm. Rec.* 26, 190-211.

[16] Laliberte AS, Winters C, Rango A. (2011): UAS remote sensing missions for rangeland applications. *Geocarto Int.* 26, 141-156.

[17] Lowe DG. (2004): Distinctive image features from scale-invariant key points. *International Journal of Computer Vision.* **2**(60), 91-110.

[18] Fischler MA, Bolles RC. (1981): Random sample consensus: A paradigm for model fitting with applications to image analysis and automated cartography. *Commun. ACM.* 24,381-395.

[19] Zhang KQ, Chen SC. (2003): A progressive morphological filter for removing nonground measurements from airborne LIDAR data. *IEEE Transactions on Geoscience & Remote Sensing.* **41**(1), 872-882.

[20] Li Y. (2013): Filtering airborne LIDAR data by an improved morphological method based on multi-gradient analysis. *ISPRS-International Archives of the Photogrammetry, Remote Sensing and Spatial Information Sciences.***XL-1/W1** (1), 191-194.

[21] Zhang WM, Qi JB, Wan P, et al. (2016): An easy-to-use airborne LIDAR data filtering method based on cloth simulation. *Remote Sensing.* **6**(8), 501.

[22] Meyer GE, Neto JC. (2008): Verification of color vegetation indices for automated crop imaging applications. *Computers & Electronics in Agriculture.* **63**(2), 282-293.

[23] Verrelst J, Schaepman ME, Koetz B, et al. (2008): Angular sensitivity analysis of vegetation indices derived from CHRIS/PROBA data. *Remoto Sensing of Environment.* **112**(5), 2341-2353.

[24] Torres SJ, Pe AJM, Castro AI, et al. (2014): Mutil-temproal mapping of the vegetation fraction in early-season wheat fields using images from UAV. *Computers and Electronics in Agriculture.* **103**, 104-113.

[25] Woebbecke DM, Meyer GE, Von BK, et al. (1993): Plant species identification, size, and enumeration using machine vision techniques on near-binary images. *Proceedings of SPIT.* **1836**, 208-219.

[26] Rango A, Laliberte A, Steele C, et al. (2006): Using unmanned aerial vehicles for rangelands: Current applications and future potentials. *Enviro. Pract*, 8, 159-168.

[27] Burnett C, Blaschke T. (2003): A multi-scale segmentation/object relationship modeling methodology for landscape analysis. *Ecol. Model.* 168, 233-249.

[28] Yu Q, Gong P, Clinton N, Biging G, Kelly M, Schirokauer D. (2006): Object-based detailed vegetation classification with airborne high spatial resolution remote sensing imagery. *Photogramm. Eng. Remote Sens.* 72, 799–811.

[29] Zhang XH, Wang XQ, Du XX, Lai JY, Xu JH. (2019): Extraction of building' seismic damage based on remote sensing images of UAV and its point clouds characteristic. *Journal of Seismological Research.* **42**(2), 230-235.

[30] Tang H, Zhai XJ, Huang W. (2018): Edge dependent Chinese restaurant process for very high resolution (VHR) satellite image over-segmentation. *10*, 1519.

[31] Li SD, Tang H, Huang X, Mao T, Niu XN. (2017): Automated detection of buildings form heterogeneous VHR satellite images for rapid response to natural disasters. *9*, 1177.

